

## Supplementary Materials for

### **PIGF-induced VEGFR1-dependent vascular remodeling determines opposing antitumor effects and drug resistance to Dll4-Notch inhibitors**

Hideki Iwamoto, Yin Zhang, Takahiro Seki, Yunlong Yang, Masaki Nakamura, Jian Wang, Xiaojuan Yang, Takuji Torimura, Yihai Cao

Published 10 April 2015, *Sci. Adv.* **1**, e1400244 (2015)  
DOI: 10.1126/sciadv.1400244

#### **This PDF file includes:**

Table S1. Sequences of the human and mouse primers used for genotyping and qPCR.

Fig. S1. PIGF protein and mRNA expression levels in human and mouse cancer cell lines.

Fig. S2. Tumor growth, microvessel density, pericyte coverage, blood perfusion and leakiness, hypoxia, tumor cell proliferation, and apoptosis of Dll4-Notch inhibitor-treated PIGF<sup>-</sup> tumors.

Fig. S3. TUNEL staining in each human and mouse tumor.

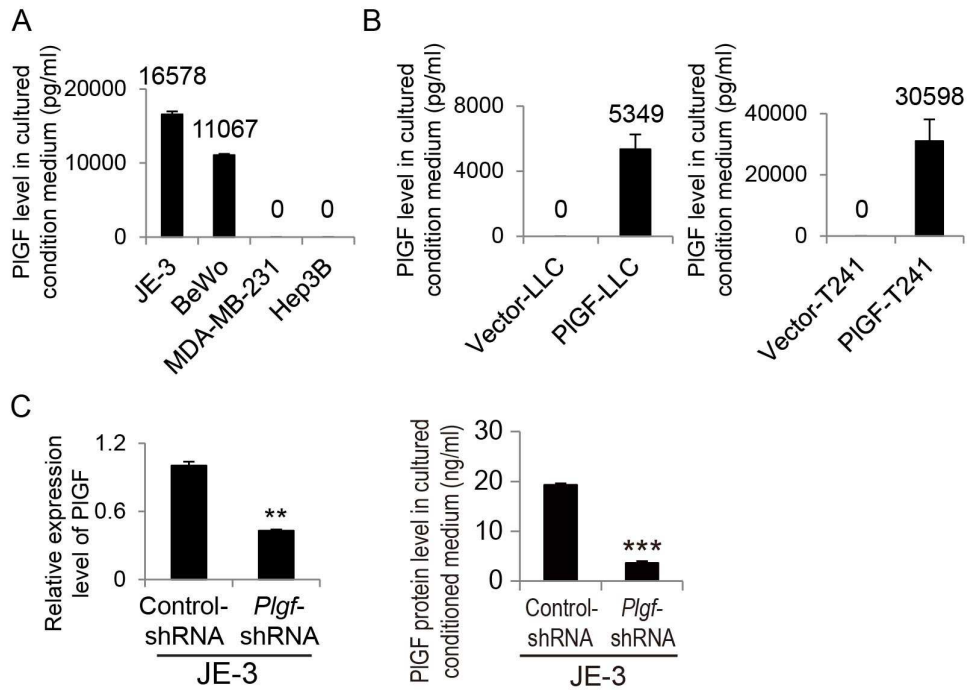
Fig. S4. Dll4-Notch inhibition–altered tumor growth and microvasculatures in mouse PIGF<sup>-</sup> and PIGF<sup>+</sup> tumors.

Fig. S5. Dll4-Notch inhibition–altered microvascular functions, tumor cell proliferation, and apoptosis in mouse PIGF<sup>-</sup> and PIGF<sup>+</sup> tumors.

## Supplementary Informartion

Genes	Species	Forward primer	Reverse primer
Vegfr1 Genotyping	mouse	5'-ACCCTCTGTACCTGGTCAATTGATGCAAAG-3'	5'-GCTAAAGCGCATGCTGCTCCAGACTGCCTTG-3' 5'-TGCAAACCTCCCACTTGCTGGCATCATAG-3'
Vegfr1	mouse	5'-CCTCACTGCCACTCTCATTGTA-3'	5'-ACAGTTTCAGGTCCTCTCCTT-3'
Vegfr2	mouse	5'-CTCATGTCTGAACTCAAGATCC-3'	5'-CCAGAATCCTCTCCATGCTCA-3'
GAPDH	mouse	5'-CCAGCAAGGACACTGAGCAA-3'	5'-GGGATGGAATTGTGAGGGA-3'
PIGF	human	5'-GTTCAAGCCATCCTGTGTCT-3'	5'-AACGTGCTGACAGAACGTC-3'
Vegfr1	human	5'-ACCATACCTCCTGCGAAACC-3'	5'-CACAGAGCCCTTCTGGTTGG-3'
Vegfr2	human	5'-CGGTCAACAACAAAGTCGGGAGA-3'	5'-CAGTGCACCACAAGACACG-3'
GAPDH	human	5'-CATTTCCTGGTATGACAACGA-3'	5'-GTCTACATGGCAACTGTGAG-3'

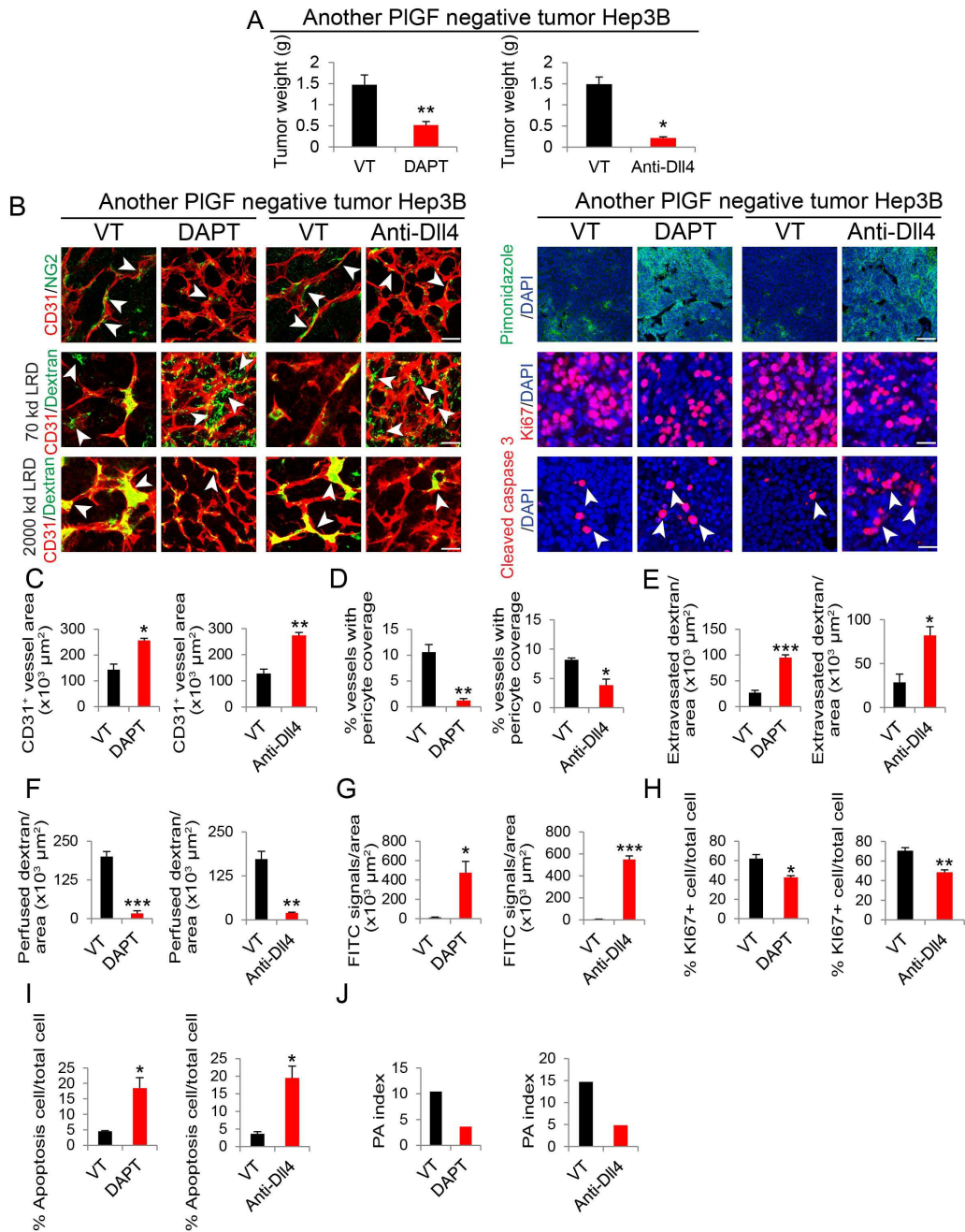
**Supplementary Table S1. Sequences of the human and mouse primers used for genotyping and qPCR.**



## Supplementary Figure 1

### Supplementary Figure S1. PIGF protein and mRNA expression levels in human and mouse cancer cell lines.

- (A) Human PIGF protein expression levels in human cancer cell lines (n = 3 independent measurements).
- (B) PIGF expression levels of mouse cancer cell lines stably expressing PIGF. Vector tumors were used as negative controls (n = 3 independent measurements).
- (C) qPCR analysis of *Plgf* mRNA expression levels (left panel) in scrambled control shRNA and *Plgf* shRNA-transfected JE-3 cells (n = 3 independent measurements). PIGF protein expression levels (right panel) in scrambled control shRNA and *Plgf* shRNA-transfected JE-3 cells (n = 3 independent measurements). The data were represented as mean determinants ( $\pm$  SEM). ; \*\*p<0.01, \*\*\*p<0.001.

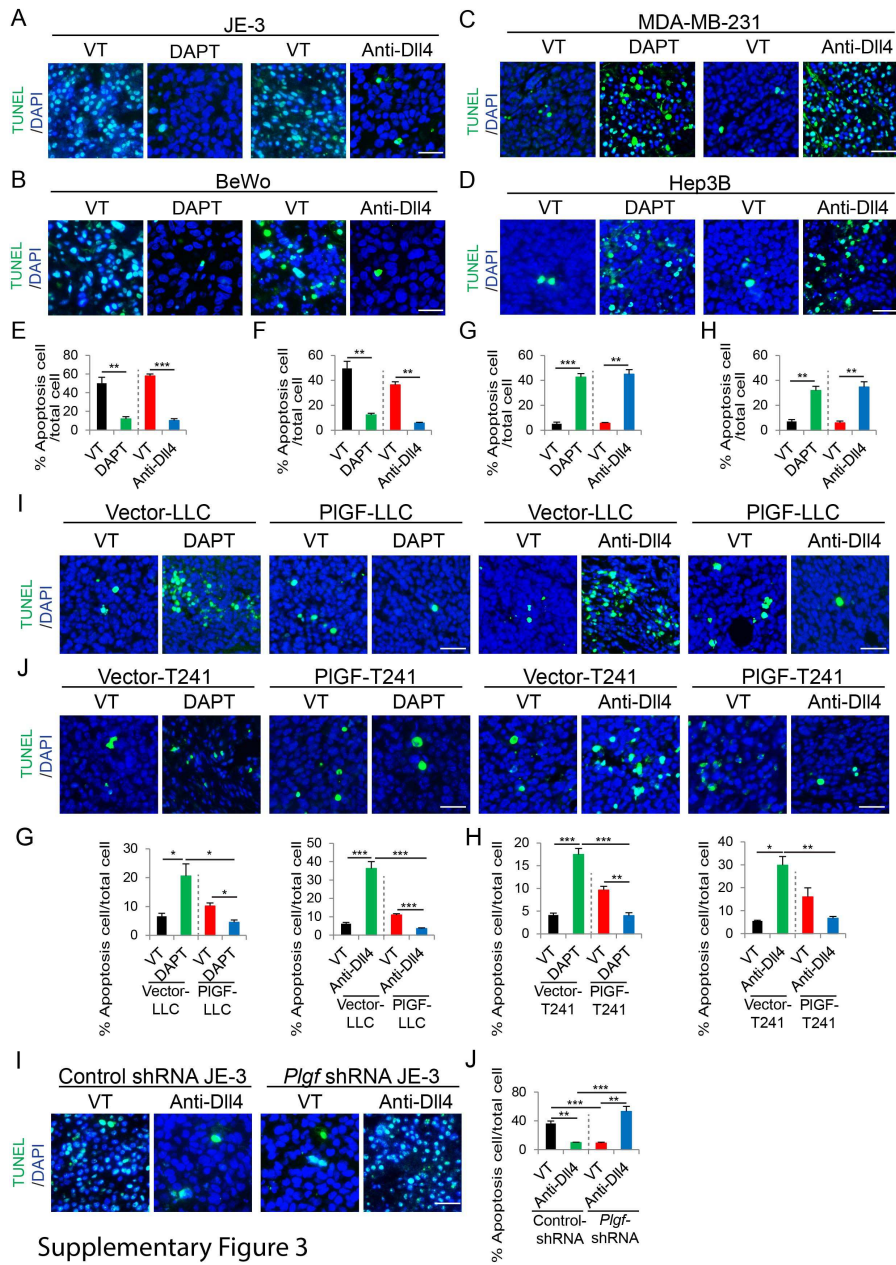


Supplementary Figure 2

**Supplementary Figure S2. Tumor growth, microvessel density, pericyte coverage, blood perfusion and leakiness, hypoxia, tumor cell proliferation, and apoptosis of Dll4-Notch inhibitor-treated PIGF<sup>-</sup> tumors.**

(A) Tumor weight of vehicle (VT)-, DAPT- and Dll4 blockade-treated Hep3B tumors (n = 6 mice/group). \*p<0.05; \*\*p<0.01

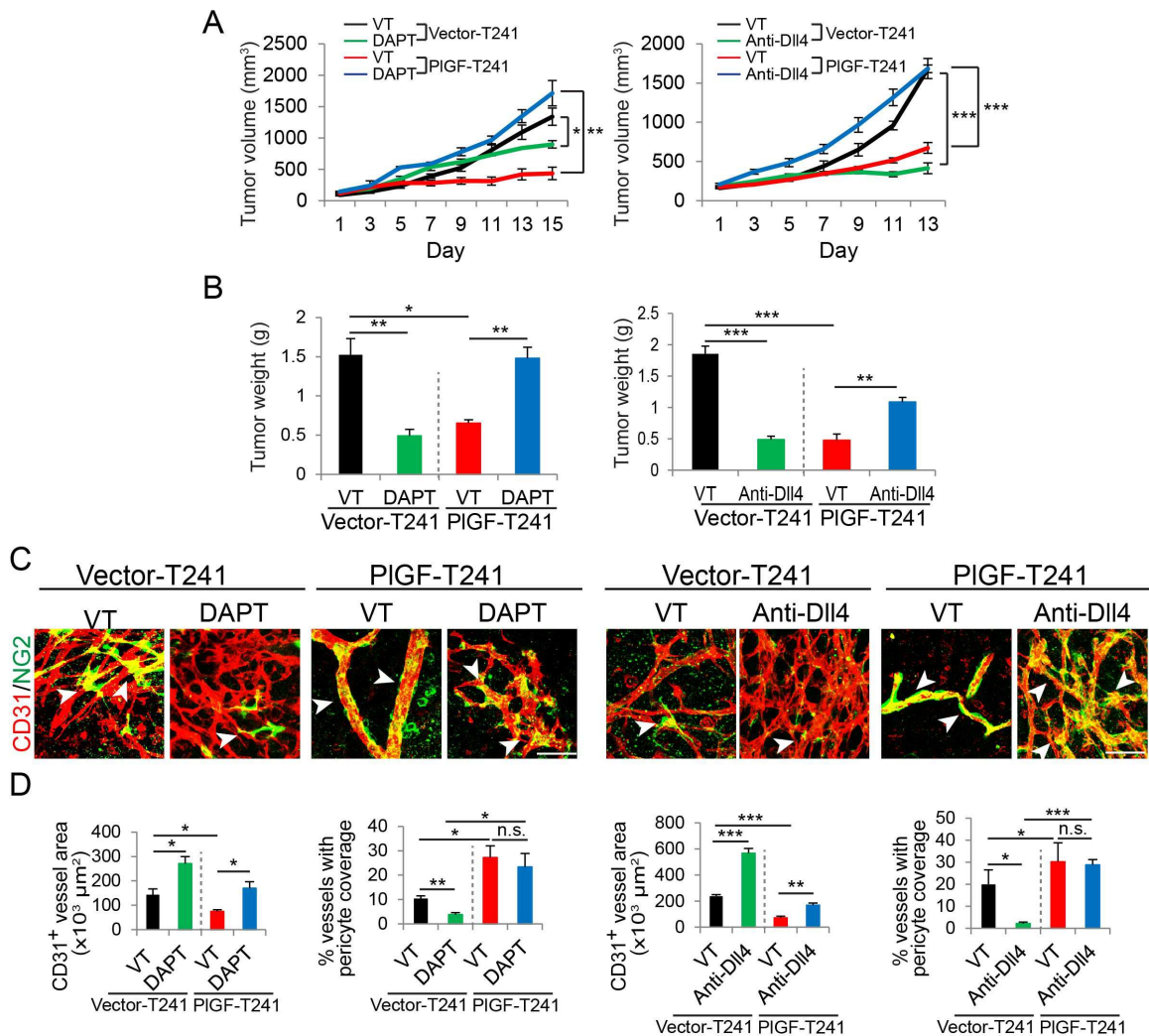
- (B) Representative images of CD31<sup>+</sup> tumor vessels, 70-kD and 2000-kD LRD, pimonidazole, Ki67, and cleaved caspase 3 in VT, DAPT and anti-Dll4 antibody-treated Hep3B tumors. Arrowheads in left upper row of panels point to pericyte coverage in tumor vessels (yellow). Arrowheads in left two low rows of panels point to extravasated 70-kD (green) or perfused 2000-kD LRD (yellow). Tumor vessels were stained with CD31 (red). Tumor hypoxia in different groups was detected with pimonidazole probe (green in the right upper row of panels, Bar = 100  $\mu$ m). Proliferating tumor cells were detected by Ki67 staining (red) and apoptotic tumor cells were detected by cleaved caspase 3 (red). Arrowheads in the right low row of panels indicated apoptotic tumor cells. Bar = 50  $\mu$ m.
- (C-J) Quantification of microvessel density and pericyte coverage, 70-kD LRD, 2000-kD LRD, pimonidazole<sup>+</sup>, Ki67<sup>+</sup>, and cleaved caspase 3<sup>+</sup> signals in VT-, DAPT- and anti-Dll4 antibody-treated Hep3B tumors (6 random fields/group). Data were presented as mean determinants ( $\pm$  SEM). Proliferation-apoptosis index (PA Index) was calculated using the formula: (% Ki67 positive cell/total cells) / (% apoptosis cells/total cell). \*p<0.05; \*\*p<0.01; \*\*\*p<0.001.



Supplementary Figure 3

**Supplementary Figure S3. TUNEL staining in each human and mouse tumor.**

(A-J) Representative images of TUNEL in VT-, DAPT- and anti-DII4 antibody-treated JE-3, BeWo, MDA-MB-231, Hep3B, vector- and PIGF-LLC, vector- and PIGF-T241, control- and *Plgf* shRNA JE-3 tumors. Quantification of tumor apoptotic cells (4-6 random fields/group) and Data represented as mean determinants ( $\pm$  SEM). \* $p < 0.05$ ; \*\* $p < 0.01$ ; \*\*\* $p < 0.001$ .



## Supplementary Figure 4

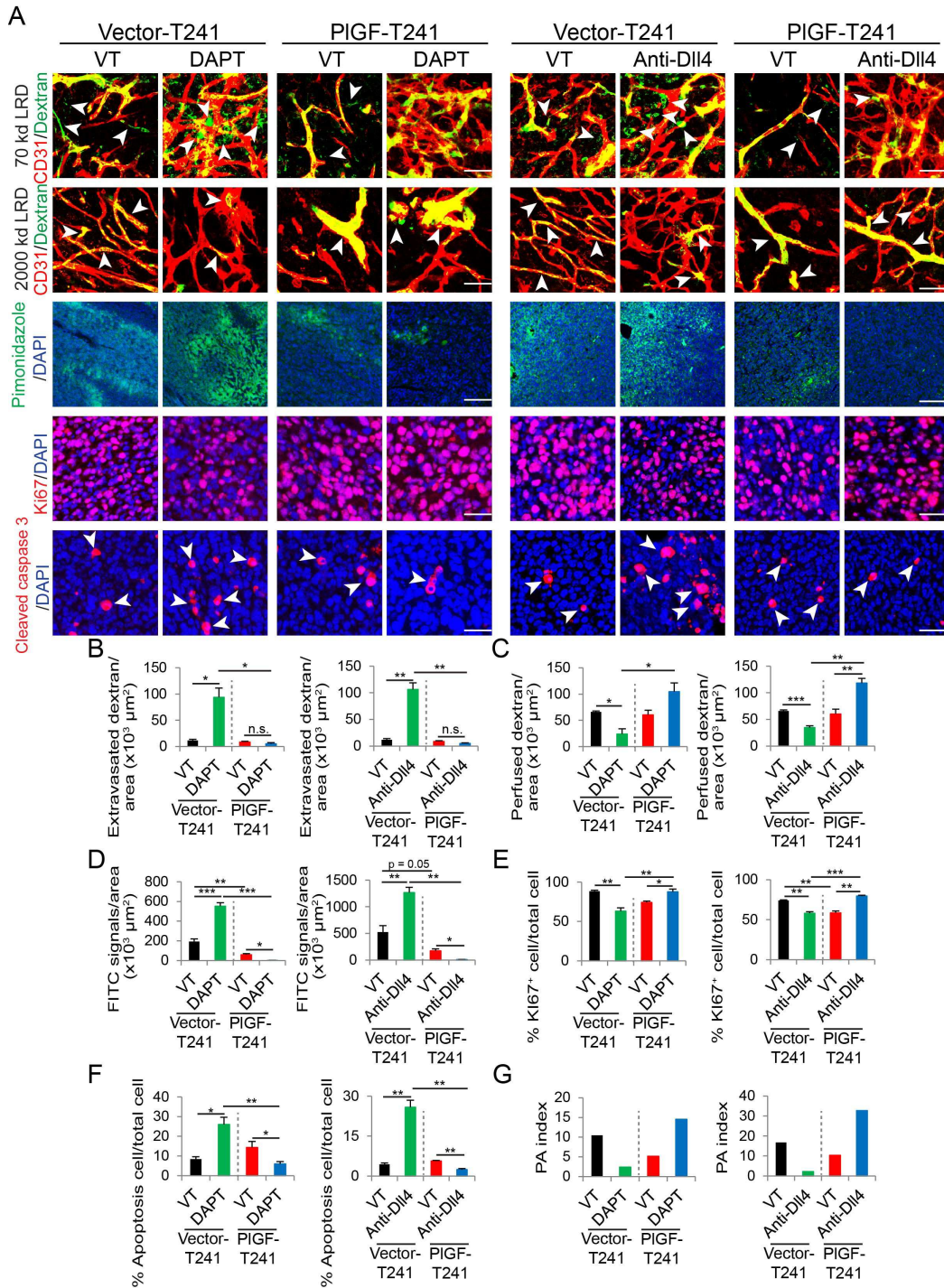
### Supplementary Figure S4. Dll4-Notch inhibition–altered tumor growth and microvasculatures in another mouse PIGF<sup>-</sup> and PIGF<sup>+</sup> tumors.

(A and B) Tumor growth rates and weights in vehicle (VT)-, DAPT- and anti-Dll4 antibody-treated vector- and PIGF-T241 tumors (6 mice/group). \*p<0.05; \*\*p<0.01; \*\*\*p<0.001.

(C and D) Representative images of CD31<sup>+</sup> tumor vessels in vehicle (VT)-, DAPT- and anti-Dll4 antibody-treated vector- and PIGF-T241 tumors. Red = CD31<sup>+</sup> signals; green = NG2<sup>+</sup> signals. Arrowheads point to pericyte coverage in tumor vessels. Bar = 50 μm. Quantification of microvessel

density and pericyte coverage in vehicle (VT)-, DAPT- and anti-Dll4 antibody-treated vector- and PlGF-T241 tumors (6 random fields/group). Data represented as mean determinants ( $\pm$  SEM). \* $p < 0.05$ ; \*\* $p < 0.01$ ; \*\*\* $p < 0.001$ ; n.s. = not significant.





Supplementary Figure 5

**Supplementary Figure S5. Dll4-Notch inhibition–altered microvascular functions, tumor cell proliferation, and apoptosis in mouse PIGF<sup>-</sup> and PIGF<sup>+</sup> tumors.**

(A) Representative images of 70-kD and 2000-kD LRD, pimonidazole, Ki67, and cleaved caspase 3 in VT, DAPT and anti-Dll4 antibody-treated

vector- and PlGF-T241 tumors. Arrowheads in upper two rows of panels point to extravasated 70-kD (green) or perfused 2000-kD LRD (yellow). Tumor vessels were stained with CD31 (red). Tumor hypoxia in different groups was detected with pimonidazole probe (green in the middle row panel). Proliferating tumor cells were detected by Ki67 staining (red) and apoptotic tumor cells were detected by cleaved caspase 3 (red). Arrowheads in the low row of panels indicated apoptotic tumor cells. Bar = 50  $\mu$ m.

(B-G) Quantification of 70-kD LRD, 2000-kD LRD, pimonidazole<sup>+</sup>, Ki67<sup>+</sup>, and cleaved caspase 3<sup>+</sup> signals in VT, DAPT and anti-Dll4 antibody-treated vector- and PlGF-241 tumors (n = 6 per group). Data were presented as mean determinants ( $\pm$  SEM). Proliferation-apoptosis index (PA Index) was calculated using the formula: (% Ki67 positive cell/total cells) / (% apoptosis cells/total cell). \*p<0.05; \*\*p<0.01; \*\*\*p<0.001.